ChemComm

Accepted Manuscript

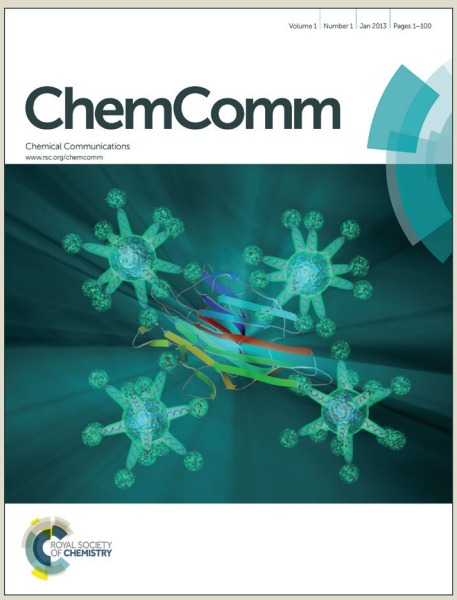

ROYAL SOCIETY OF CHEMISTRY

www.rsc.org/chemcomm

Cite this: DOI: 10.1039/c0xx00000x

www.rsc.org/xxxxxx

ARTICLE TYPE

Sensitive detection of transcription factors with Ag^+-stabilized self-assembly triplex DNA molecular switch

Desong Zhu,[a] Jing Zhu,[a] Ye Zhu,[a] Lei Wang*[b] and Wei Jiang*[a]

Received (in XXX, XXX) Xth XXXXXXXXX 20XX, Accepted Xth XXXXXXXXX 20XX
DOI: 10.1039/b000000x

Based on a Ag^+-stabilized self-assembly triplex DNA molecular switch (Ag^+-STDMS), a simple, enzyme-free and sensitive new fluorescent strategy for detection of transcription factors was developed, achieving high sensitivity towards purified targets and real biological samples.

Transcription factors (TFs) are sequence specific DNA-binding proteins that modulate the process of gene transcription by binding to specific double-stranded DNA (dsDNA) sequences.[1] Their expression levels sensitively reflect cellular development stage and disease state. It is generally recognized that TFs usually keep relatively low concentration in the early stage of diseases. Therefore, the sensitive detection of TFs is crucial for early diagnosis of diseases and drugs development.[2] So far, many strategies have been exploited for the detection of TFs, such as electrophoresis mobility shift assay (EMSA),[3] enzyme-linked immunosorbent assay (ELISA)[4] and electrochemical strategies.[5,6] However, there are still some shortcomings. For EMSA and ELISA, the involvements of radioisotope labels and specific antibodies against each TF lead to a potential security risk and narrow application scope. For electrochemical strategies, the complicated electrode modification processes are generally laborious and time-consuming.

Alternatively, fluorescence-based strategies have been exploited for the detection of TFs because of safety, simpleness and high sensitivity.[7] To date, fluorescence-based strategies are roughly divided into two categories. The first is based on the conformation change of dsDNA recognition probes.[8-10] Typically, two short duplexes containing half of the protein-binding site are labeled with a fluorescence donor and an acceptor, respectively. In the presence of TFs, the association of the two short duplexes results in a 'switch-on' fluorescence resonance energy transfer (FRET) signal.[8] Another example is a double stem-loop structure molecular beacon in which quencher is labeled in the middle of the DNA sequence. In the presence of TFs, the conformation equilibrium shift of molecular beacons from double stem-loop to single stem-loop results in a 'switch-off' FRET signal.[9] The detection of TFs amenable to the first strategy involves the complicated procedures in designing the proper two short duplexes and the double stem-loop molecular beacons, which limits the broad application of this strategy. The second is based on the exonuclease or the endonuclease protection.[11-14] TFs

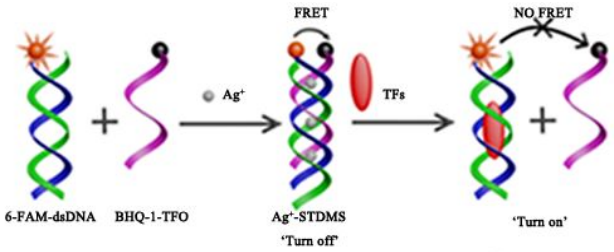

Scheme 1. Schematic illustration of sensitive detection of transcription factors with Ag^+-STDMS.

specifically bind to the dsDNA recognition probes, which hinders the exonuclease or the endonuclease from approaching the recognition probes and protects the recognition probes from being continually digested.[11-14] This strategy shows a high sensitivity. Nevertheless, due to the requirement of the additional enzymes, it is susceptible to false positives caused by non-specific protein binding.[10] Moreover, the small changes of reaction conditions, such as temperature, pH and the buffer solution composition also can weaken the activity of enzymes, leading to a decreased sensitivity. In addition, for the analysis of the endogenous TFs in real biological samples, the endogenous nucleases may influence the activity of the enzymes added in the detection process, which leads to unsatisfactory results.[15] In consideration of the above limitations, the development of new fluorescent strategy for simple, enzyme-free and sensitive detection of TFs, is highly desirable.

Recently, the triplex DNA has become one of the most attractive recognition motifs in the designs of strategies for sequence-specific labeling, regulating gene expression and constructing DNA-based nanostructures.[16-20] Among those designs, the sequence-specific recognition of double-stranded DNA is realized by constructing a triplex DNA.[19] Another typical example is continuous assays for DNA translocation using fluorescent triplex DNA dissociation.[20]

Inspired by the application of the triplex DNA, we developed a simple, enzyme-free and sensitive new fluorescent strategy for the detection of TFs based on a Ag^+-stabilized self-assembly triplex DNA molecular switch (Ag^+-STDMS). As a proof of the concept, NF-κB p50, a cancer-related TF, was chosen as a model in our experiments. As shown in Scheme 1, the dsDNA and the triplex-forming oligonucleotide (TFO) were labeled with a

Table 1 Sequences of oligonucleotides

Name	Sequences
DNA-1	3'- TTT TT T TT **CCC TT TCAGGG** GAGTA-5'
DNA-2	5'-6-FAM-AAAAA AAA G**GGAA AGTCCC** C TCAT-3'
TFO-1 (12-mer)	5'-BHQ-1- TTT TT T TT CCC T-3'
TFO-2 (15-mer)	5'-BHQ-1- TTT TT T TT CCC T T TC-3'
TFO-3 (18-mer)	5'-BHQ-1- TTT TT T TT CCC T T TC TCC-3'

The boldface regions denote the binding sequence of NF-κB p50. The underlined regions denote the components of the triplex DNA.

The 12-mer, 15-mer and 18-mer denote the number of bases of three BHQ-1-TFO.

fluorophore (6-FAM) and a quencher (BHQ-1), respectively. They were denoted as 6-FAM-dsDNA and BHQ-1-TFO. All oligonucleotides were listed in Table 1. The 6-FAM-dsDNA contained NF-κB p50 recognition sequence that partially overlapped the homopyrimidine strand with BHQ-1-TFO. The TFO binds to the dsDNA by Hoogsteen bond to form the triplex DNA containing C•G◦C and T•A◦T triads (• denotes Hoogsteen bond, ◦ denotes Watson-Crick bond).[21-23] Ag^+ can specifically recognize the C•G◦C triads to form AgC•G◦C and enhance the stability of triplex DNA.[24] Therefore, with the aid of Ag^+, the self-assembly process of the BHQ-1-TFO binding to the 6-FAM-dsDNA occurred to form Ag^+-STDMS containing AgC•G◦C and T•A◦T triads. The self-assembly made BHQ-1-TFO and 6-FAM-dsDNA approach each other. As a result, the fluorescence of 6-FAM-dsDNA was quenched by FRET. Because the affinity of NF-κB p50 for 6-FAM-dsDNA was much stronger than that of BHQ-1-TFO for 6-FAM-dsDNA,[25,26] in the presence of NF-κB p50, the NF-κB p50 bound to 6-FAM-dsDNA and displaced the BHQ-1-TFO, resulting in the separation of BHQ-1-TFO from 6-FAM-dsDNA and the fluorescence restoration of 6-FAM-dsDNA. In this way, NF-κB p50 could be quantified very simply and sensitively by fluorescence restoration of 6-FAM-dsDNA.

The feasibility of the proposed strategy was confirmed by the fluorescence plectrums of the 6-FAM-dsDNA under different conditions. As shown in Fig. 1, the 6-FAM-dsDNA showed a strong fluorescence intensity (curve a) and there was almost no change after addition of Ag^+ (curve b). When a 15-mer BHQ-1-TFO was added into 6-FAM-dsDNA solution without Ag^+, the fluorescence intensity decreased slightly, which indicated the formation of a small number of triplex DNA (curve c). However, when 15-mer BHQ-1-TFO was added into the system containing 6-FAM-dsDNA and Ag^+, the fluorescence intensity decreased significantly, which indicated that the formation of a large number of triplex DNA (curve d). This phenomenon showed that Ag^+ was able to improve the stability of the triplex DNA, which was consistent with the previous report.[24] And then, when NF-κB p50 was added into the above system, the fluorescence intensity increased dramatically, which attributed to the displacement of BHQ-1-TFO by NF-κB p50 and the separation of BHQ-1-TFO from 6-FAM-dsDNA (curve e). In addition, the UV melting curves of the triplex DNA were also investigated under different conditions (see Fig. S5, ESI†). In the absence of Ag^+, the melting temperature of the triplex DNA was 33 °C (Tm=33 °C when using 15-mer BHQ-1-TFO). However, in the presence of Ag^+, the

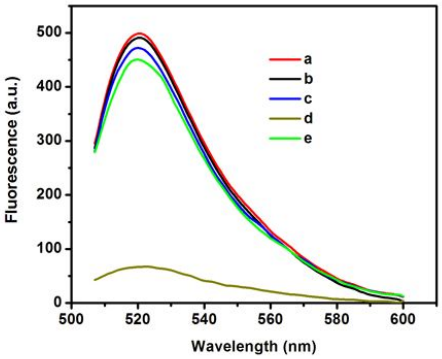

Fig. 1 The fluorescence spectras of the 6-FAM-dsDNA under different conditions.
(a) 6-FAM-dsDNA, (b) 6-FAM-dsDNA + Ag^+, (c) 6-FAM-dsDNA + BHQ-1-TFO (15-mer), (d) 6-FAM-dsDNA + BHQ-1-TFO (15-mer) + Ag+ , (e) 6-FAM-dsDNA + BHQ-1-TFO (15-mer) + Ag^+ + NF-κB p50. Experimental conditions: 10 mM of PBS (pH 7.4), 200 mM of $NaNO_3$, 50 nM of 6-FAM-dsDNA, 500 nM of BHQ-1-TFO, 20 μM of Ag^+, 0.55 nM of NF-κB p50, 30 minutes of self-assembly at 37 °C, 10 minutes of displacement at 37 °C. The excitation and emission wavelengths were set at 495 and 518 nm, respectively.

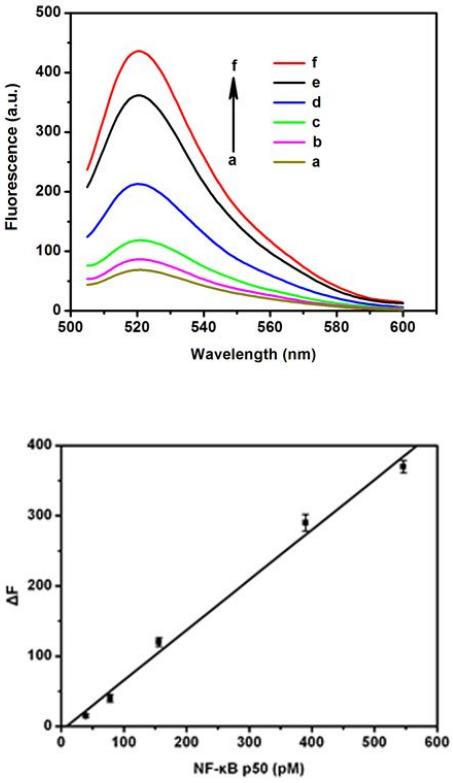

Fig. 2 The fluorescence spectrums with increasing concentration of NF-κB p50 (above) and the relationship between fluorescence intensity and the concentration of NF-κB p50 (below). The error bars showed the standard deviation of three replicate determinations. Experimental conditions: 10 mM of PBS (pH 7.4), 200 mM of $NaNO_3$, 50 nM of 6-FAM-dsDNA, 500 nM of BHQ-1-TFO (15-mer), 20 μM of Ag^+, target (a to f): 0, 40, 80, 160, 400 and 550 pM, respectively. 30 minutes of self-assembly at 37 °C, 10 minutes of displacement at 37 °C. The excitation and emission wavelengths were set at 495 nm and 518 nm, respectively.

melting temperature was 57 °C (Tm2=57 °C when using 15-mer BHQ-1-TFO). The remarkable rise of Tm further substantiated the stabilization effect of Ag^+ on the triplex DNA.

In order to achieve the best sensing performance of this system, keeping high stability of Ag^+-STDMS was especially important. So, the effect of the concentration of Ag^+ was investigated firstly (see Fig. S1, ESI†). It was estimated with the change of fluorescence intensity, which was defined as $\Delta F = F - F0$ (F denotes fluorescence intensity in the presence of target and F0 denotes the fluorescence intensity in the absence of target). The ΔF increased along with the increase of Ag^+ concentration and reached a plateau after 20 μM, which demonstrated that Ag^+ indeed improved the stability of triplex DNA. However, ΔF decreased gradually when the concentration of Ag^+ was higher than 20 μM, which might be due to the formation of the C-Ag-C complex through the interaction between Ag^+ and TFO in the presence of excess Ag^+. As a result, 20 μM of Ag^+ was chosen for the further research. The effects of other experimental parameters including the length of the BHQ-1-TFO, the concentration of the BHQ-1-TFO and pH were also investigated (see Fig. S2–S4, ESI†). The optimal conditions were 20 μM of Ag^+, 15-mer BHQ-1-TFO, 500 nM of BHQ-1-TFO and pH 7.4. The sensitivity and linear range were evaluated with varying NF-κB p50 concentrations. As shown in Fig. 2, the ΔF increased proportionally to the target concentration from 40 pM to 550 pM. The linear regression equation was $\Delta F = 0.71C - 5.79$ (C: pM, $R^2 = 0.992$) and the limit of detection (LOD) was 25 pM (3σ/slope), which was superior to some reported methods (see Table S1, ESI†). The relative standard deviation (RSD) was 5.7% for 550 pM NF-κB p50 (n = 5).

The specificity of the proposed strategy was studied by evaluating the degree of the nonspecific binding of interfering proteins under the same experimental conditions as in the case of NF-κB p50. As shown in Fig. 3, the fluorescence intensities for human thrombin, human IgG and BSA were much lower than that for NF-κB p50. Moreover, the fluorescence intensity for mixed sample consisting of NF-κB p50, human thrombin, human IgG and BSA was comparable to that for only NF-κB p50. These results clearly demonstrated the high specificity of the proposed strategy for NF-κB p50 detection.

Initially, NF-κB p50 is bound to the inhibitory protein IκB and is unactivated in the cytoplasm. In the presence of activators, such as cytokines, bacterial and viral products, NF-κB p50 is released from the IκB into the nucleus and becomes activated.[27] The tumor necrosis factor-α (TNF-α) is used to activate the NF-κB p50 in HeLa cell and the activated NF-κB p50 enters the HeLa cell nucleus.[28] Therefore, to further demonstrate the capability of the proposed strategy for the real sample, the activated NF-κB p50 in TNF-α-treated HeLa cell nuclear extracts was measured. As shown in Fig. 4, Two large fluorescence intensity variances were observed in the untreated nuclear extracts spiked with NF-κB p50 (curve a) and TNF-α-treated nuclear extracts (curve b). However, the untreated cell nuclear extracts displayed a negligible fluorescence intensity variance (curve c) as compared with the control without the nuclear extracts (curve d). These results fully confirmed the capability of the proposed strategy for the detection of NF-κB p50 in the real sample. Moreover, for real sample, the calibration curve and the

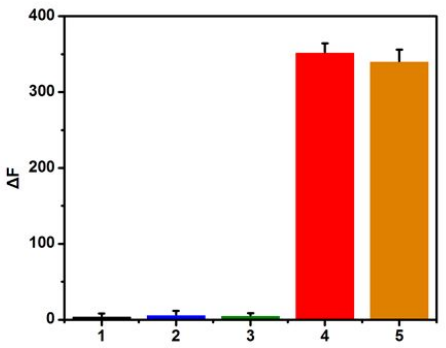

Fig. 3 The specificity of the proposed strategy. (1) human thrombin, (2) human IgG, (3) BSA, (4) NF-κB p50, (5) mixed sample. The error bars showed the standard deviation of three replicate determinations. Experimental conditions: 10 mM of PBS (pH 7.4), 200 mM of $NaNO_3$, 50 nM of 6-FAM-dsDNA, 500 nM of BHQ-1-TFO (15-mer), 20 μM of Ag^+, 50 nM of interfering proteins (human thrombin, human IgG, BSA and mixed sample), 0.55 nM of NF-κB p50, 30 minutes of self-assembly at 37 °C, 10 minutes of displacement at 37 °C. The excitation and emission wavelengths were set at 495 and 518 nm, respectively.

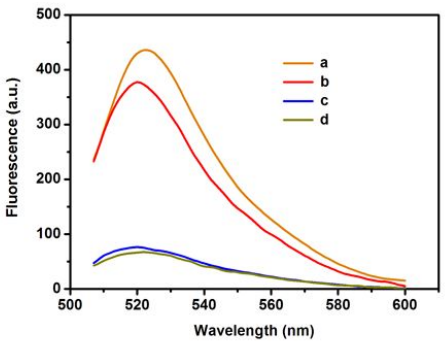

Fig. 4 The fluorescence spectrums of the NF-κB p50 in the real samples. (a) untreated nuclear extracts (25 ng/μL) spiked with NF-κB p50 (0.55 nM), (b) TNF-α-treated nuclear extracts (25 ng/μL), (c) untreated nuclear extracts (25 ng/μL), (d) the control without the nuclear extracts. Other experimental conditions: 10 mM of PBS (pH 7.4), 200 mM of $NaNO_3$, 50 nM of 6-FAM-dsDNA, 500 nM of BHQ-1-TFO (15-mer), 20 μM of Ag^+, 30 minutes of self-assembly at 37 °C, 10 minutes of displacement at 37 °C. The excitation and emission wavelengths were set at 495 and 518 nm, respectively.

detection limit were also obtained. As shown in Fig. S6, the ΔF increased proportionally to the target concentration from 1 ng/μL to 25 ng/μL. The linear regression equation was $\Delta F = 12.6C + 6.8$ (C: ng/μL, $R^2 = 0.992$) and the limit of detection (LOD) was 0.8 ng/μL (3σ/slope).

Conclusions

In summary, taking advantage of a Ag^+-STDMS, we developed a simple, enzyme-free and sensitive new fluorescent strategy for the detection of NF-κB p50. Compared with the fluorescent strategies mentioned above, it possessed of unique and attractive

characteristics: (i) A Ag^+-STDMS as a bifunctional probe that could recognize targets and carry signals was firstly introduced into the detection of TFs. Moreover, with the aid of Ag^+, this new bifunctional probe could be easily synthesized and show high stability without the need of any other stabilizers. (ii) Because this proposed strategy did not involve any enzyme, the false positives caused by non-specific protein binding and the negative effect of the endogenous nuclease in the real samples could be eliminated. (iii) It was potentially universal because this Ag^+-STDMS could be easily designed for other targets by simply changing the corresponding recognition sequence. Moreover, this proposed strategy showed not only high sensitivity with the detection limit of purified recombinant NF-κB p50 as low as 25 pM , but also excellent performance for the real biological sample assays. Finally, this strategy not only offered a highly sensitive sensing platform for early diagnosis of cancers and other similar diseases, but also opened up an exciting new avenue for a wide range of the detection techniques.

This work was supported by National Natural Sciences Foundation of China (No. 21175081, 21175082, 21375078 and 21475077).

Notes and references

[a] *Key Laboratory for Colloid and Interface Chemistry of Education Ministry, Department of Chemistry, Shandong University, Jinan, 250100, China. E-mail: wjiang@sdu.edu.cn; Fax: +86 531 88564464; Tel: +86 531 88362588.*

[b] *School of Pharmacy, Shandong University, Jinan 250012, P.R. China. E-mail: wangl-sdu@sdu.edu.cn; Tel: +86 531 88380036.*

† Electronic Supplementary Information (ESI) available: Materials and additional detials for the experiment procedure and supplementary figures. See DOI: 10.1039/b000000x/

1 A. G. N. Papavassiliou, *Engl. J. Med*. 1995, **332**, 45−47.
2 P. P. Pandolfi, *Oncogene*, 2001, **20**, 3116−3127.
3 M. M. Garner, A. Revzin, *Nucleic Acids Res*., 1981, **9**, 3047–3060.
4 P. Renard, I. Ernest, A. Houbion, M. Art, H. Le Calvez, M. Raes, J. Remacle, *Nucleic Acids Res*., 2001, **29**, e21.
5 J. Wang, W. W. Zhao, X. R. Li, J. J. Xu, H. Y. Chen, *Chem. Commun*., 2012, **48**, 6429–6431.
6 J. Wang, W. W. Zhao, H. Zhou, J. J. Xu, H. Y. Chen, *Biosens. Bioelectron.*, 2013, **41**, 615–620.
7 J. J. Hill and C. A. Royer, *Methods Enzymol*., 1997, **278**, 390–416.
8 T. Heyduk and E. Heyduk, *Nat. Biotechnol*., 2002, **20**, 171–176.
9 A. Vallee-Belisle, A. J. Bonham, N. O. Reich, F. Ricci and K. W. Plaxco, *J. Am. Chem. Soc*., 2011, **133**, 13836–13839.
10 J. J. Liu, X. R. Song, Y. W. Wang, G. N. Chen and H. H. Yang, *Nanoscale*, 2012, **4**, 3655–3659.
11 J. K. Wang, T. X. Li, X. Y. Guo and Z. H. Lu, *Nucleic Acids Res*., 2005, **33**, e23.
12 H. J. He, R. Pires, T. N. Zhu, A. H. Zhou, A. K. Gaigalas, S. G. Zou and L. L. Wang, *BioTechniques*, 2007, **43**, 93–98.
13 X. F. Liu, L. Ouyang, X. H. Cai, Y. Q. Huang, X. L. Feng, Q. L. Fan, W. Huang, *Biosens. Bioelectron*., 2013, **41**, 218−224.
14 A. Cao, C. Y. Zhang, *Anal. Chem.*, 2013, **85**, 2543−2547.
15 C. Wu, *Nature*, 1984, **309**, 229−234.
16 Y. Chen, S. H. Lee, and C. D. Mao, *Angew. Chem., Int. Ed.*, 2004, **43**, 5335–5338.
17 J. Tumpane, R. Kumar, E. P. Lundberg, P. Sandin, N. Gale, I. S. Nandhakumar, B. Albinsson, P. Lincoln, L. M. Wilhelmsson, T. Brown, et al., *Nano Lett.*, 2007, **7**, 3832–3839.
18 Y. Takezawa, W. Maeda, K. Tanaka and M. Shionoya, *Angew. Chem., Int. Ed.*, 2009, **48**, 1081–1084.
19 Z. Y. Xiao, X. T. Guo, L. S. Ling, *Chem. Commun.,* 2013, **49**, 3573–3575.
20 S. E. McClelland, D. T. Dryden and M. D. Szczelkun, *J. Mol. Biol.*, 2005, **348**, 895–915.
21 Y. Chen, S. H. Lee, and C. D. Mao, *Angew. Chem., Int. Ed.*, 2004, **43**, 5335–5338.
22 J. Tumpane, R. Kumar, E. P. Lundberg, P. Sandin, N. Gale, I. S. Nandhakumar, B. Albinsson, P. Lincoln, L. M. Wilhelmsson, T. Brown, et al., *Nano Lett.*, 2007, **7**, 3832–3839.
23 Y. Takezawa, W. Maeda, K. Tanaka and M. Shionoya, *Angew. Chem., Int. Ed.*, 2009, **48**, 1081–1084.
24 T. Ihara, T. Ishii, N. Araki, A. W. Wilson and A. Jyo, *J. Am. Chem. Soc.*, 2009, **131**, 3826–3827.
25 M. B. Urban, P. A. Baeuerle, *genes & development*, 1990, **4**, 1975-1984.
26 L. J. Maher, III, P. B. Dervan, and B. J. Wold, *Biochemistry*, 1990, **29**, 8820-8826.
27 F. Chen, V. Castranova, X. Shi, L. M. Demers, *Clin. Chem.*, 1999, **45**, 7-17.
28 J. A. DiDonato, M. Hayakawa, D. M. Rothwarf, E. Zandi, and M. Karin, *Nature*, 1997, **388**, 54−554.